Preprints of the 21st IFAC World Congress (Virtual)
Berlin, Germany, July 12-17, 2020

Synchronization of a swarm of unicycle robots using dynamic control ⋆

I. Ruiz-Ramos * **A. Morales** ** **J. Pena Ramirez** ***

* *Robotics and Advanced Manufacturing Program CINVESTAV Coahuila-Saltillo (e-mail: isaac.ruiz0988@ gmail.com)*
** *Robotics and Advanced Manufacturing Program CINVESTAV Coahuila-Saltillo (e-mail: america.morales@ cinvestav.edu.mx)*
*** *Research Center for Science and Higher Education at Ensenada, Baja California, Mexico (e-mail: jpena@cicese.com)*

Abstract:
This paper proposes a dynamic controller for a swarm of unicycle robots following a desired trajectory and maintaining a prescribed formation. Furthermore, a comparison of the proposed dynamic controller versus a traditional static feedback controller is presented.The stability analysis of the closed loop system is determined by using the Lyapunov stability theory and the theoretical results are numerically illustrated. Also a comparison in terms of energy, between the proposed dynamic controller and the classical static feedback controller is provided.

Keywords: Mobile robot, dynamic coupling, diffuse coupling, synchronization

1. INTRODUCTION

There are several works addressing the multi-agent coordination problem, from which two approaches can be distinguished: centralized and decentralized schemes. In a centralized scheme, there is a central computer which computes the control laws and send them to the involved agents. On the other hand, in a decentralized scheme, each agent has its own computer on board to calculate the corresponding control law and also to communicate with other agents.

There are also different directions which sometimes they overlap to offer better solutions; two of these directions are: consensus and distributed formation, see (Cao et al., 2013). In consensus, all the agents reach to a common agreement, see (Olfati and Murray, 2004). On the other hand, in distributed formation, all the agents form a geometrical pre-designed figure through local interactions, see (Pavone and Frazzoli, 2007) and (Ren, 2009). We use these directions in this work, but our main direction is consensus. In this context, synchronization appears as a solution to keep a coordination between the agents or systems. To achieve this, it is essential that the agents in the network communicate each other by a channel, which is called coupling, which can be either static or dynamic.

The static couplings are constructed with the weighted differences between the states of the involved systems, i.e. in this case the interaction between the agents is direct, see e.g. (van de Wouw et al., 2017). This coupling is often used to synchronize pairs or groups of systems, see e.g. (Gutierrez et al., 2017), (Morales and Nijmiejer, 2016), and (Pereira et al., 2014).

On the other hand, when the coupling is dynamic, then the interaction between the agents in the network is indirect. Furthermore, the behavior of the coupling signal is governed by a dynamical system, cf. (Suykens et al., 1997).

According to (Pena Ramirez et al., 2018), both couplings have their own advantages and disadvantages. The static couplings have the advantage that its implementation is relatively easy but, for certain systems, this type of coupling fails to induce synchronization or synchronization can be induced in the network only for a narrow interval of coupling strength values. On the other hand, a dynamic coupling seems to solve these limitations but this type of coupling requires to increase the number of equations at each node.

In this work we present the design of a novel dynamic controller for inducing synchronized/cooperative behavior in a swarm of unicycle robots. The proposed controller is based on our previous work (Gutierrez et al., 2017), were the derived controller was static. The stability of the closed-loop system is formally studied and a comparison of the obtained results to those obtained when using the static controller are provided. The outcome of the comparison suggest that the energy consumption of the proposed controller is smaller than the consumption of the static controller.

The outline of the paper is as follows. First, the mathematical preliminaries and the problem statement are presented in Section 2. Next, Section 3 introduces the proposed controller, and then in Section 4, the performance of the controller is numerically investigated. Finally, some conclusions are presented in Section 5.

⋆ This research has been supported by Mexican Council for Science and Technology (CONACYT).

2. PRELIMINARIES AND PROBLEM STATEMENT

Consider a network composed by N unicycle robots, which keep a formation via a virtual structure scheme. The kinematic model describing the time evolution of each agent in the network is given by

$$\dot{\mathbf{q}}_i = \begin{bmatrix} \cos\theta_i & 0 \\ \sin\theta_i & 0 \\ 0 & 1 \end{bmatrix} \begin{bmatrix} v_i \\ \omega_i \end{bmatrix}, \tag{1}$$

where $\mathbf{q}_i(t) = [x_i(t), y_i(t), \theta_i(t)]^T$ is the pose of each robot respect to a global reference frame (GRF), the control inputs v_i and ω_i are the linear and angular velocities of the robot, respectively. Furthermore, each robot has the following well-known nonholonomic constraint

$$\dot{y}_i \cos\theta_i - \dot{x}_i \sin\theta_i = 0, \tag{2}$$

which implies that the unicycle can only move forwards and backwards.

The main idea of the virtual structure is that a swarm of N agents keeps a formation where each one has a position, $\mathbf{p}_i = [p_i^x, p_i^y]^T$ $(i = 1, \ldots, N)$, see Fig. 1, with respect to the virtual center (VC) of the formation meanwhile the VC follows a desired trajectory respect to the GRF. This desired trajectory is denoted by the orange dashed line in Fig. 1 and is given by $\mathbf{q}_{vc} = [x_{vc}^r, y_{vc}^r, \theta_{vc}^r]^T$, where x_{vc}^r and y_{vc}^r are the position of the VC on the x and y axis, respectively, and θ_{vc}^r the orientation of the virtual structure.

According to (Gutierrez et al., 2017), there is a procedure for designing the control signals v_i and ω_i for each robot. In what follows we briefly summarize the procedure.

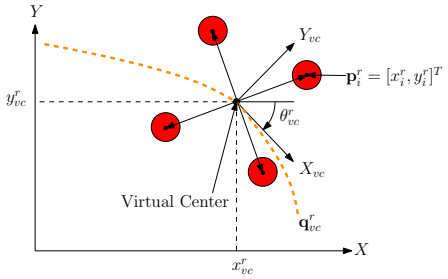

Fig. 1. Virtual structure scheme. The robots are located in positions respect to the virtual center (VC).

The reference trajectory, $\mathbf{q}_i^r(t) = [x_i^r(t), y_i^r(t), \theta_i^r(t)]^T$ $(i = 1, \ldots, N)$, for each robot with respect to the GRF, is given by

$$\mathbf{q}_i^r(t) = \begin{bmatrix} \mathbf{p}_i^r(t) \\ \theta_i^r \end{bmatrix} = \begin{bmatrix} \mathbf{p}_{vc}^r(t) + \mathbf{R}(\theta_{vc}^r)\mathbf{p}_i \\ \arctan\left(\dfrac{\dot{y}_i^r}{\dot{x}_i^r}\right) \end{bmatrix}, \tag{3}$$

where $\mathbf{p}_i^r(t) = [x_i^r, y_i^r]^T$ is the reference position of each robot, $\mathbf{p}_{vc}^r(t) = [x_{vc}^r, y_{vc}^r]^T$ is the position of the VC respect to GRF and $\mathbf{R}(\theta_{vc}^r) \in R^{2\times 2}$ is a rotational matrix which is given by

$$\mathbf{R}(\theta_{vc}^r) = \begin{bmatrix} \cos\theta_{vc}^r & -\sin\theta_{vc}^r \\ \sin\theta_{vc}^r & \cos\theta_{vc}^r \end{bmatrix}. \tag{4}$$

In Eq. (3) the orientation (θ_i^r) of each robot depends on the reference velocities on each axis. This velocities can be obtained by

$$\dot{\mathbf{p}}_i^r = \dot{\mathbf{p}}_{vc}^r + \dot{\theta}_{vc}^r \mathbf{S}\mathbf{R}(\theta_v c^r)\mathbf{p}_i, \ i = 1, \ldots, N, \tag{5}$$

where $\mathbf{S}$ is a 2×2 skew-symmetric matrix given by

$$\mathbf{S} = \begin{bmatrix} 0 & -1 \\ 1 & 0 \end{bmatrix}. \tag{6}$$

Solving (2) for θ_i and comparing to (3), it can be seen that the reference trajectory for each robot has the same constrain for the unicycle. Therefore, each trajectory has the same kinematic model for the unicycle, i.e.

$$\dot{\mathbf{q}}_i^r = \begin{bmatrix} \cos\theta_i^r & 0 \\ \sin\theta_i^r & 0 \\ 0 & 1 \end{bmatrix} \begin{bmatrix} v_i^r \\ \omega_i^r \end{bmatrix}, \ i = 1, \ldots, N. \tag{7}$$

This implies that we need to know the reference velocities v_i^r and ω_i^r. This velocities can be obtained by

$$v_i^r = \|\dot{\mathbf{p}}_i^r\|_2, \ \omega_i^r = -\frac{\langle \dot{\mathbf{p}}_i^r, \mathbf{S}\ddot{\mathbf{p}}_i^r \rangle}{\langle \dot{\mathbf{p}}_i^r, \dot{\mathbf{p}}_i^r \rangle}, \ i = 1, \ldots, N, \tag{8}$$

where $\dot{\mathbf{p}}_i^r$ and $\mathbf{S}$ are defined in (5) and (6), respectively, and

$$\ddot{\mathbf{p}}_i^r = \ddot{\mathbf{p}}_{vc}^r + \left(\ddot{\theta}_{vc}^r \mathbf{S} - \left(\dot{\theta}_{vc}^r\right)^2 \mathbf{I}^{2\times 2}\right) \mathbf{R}(\theta_{vc}^r)\mathbf{p}_i, \tag{9}$$

for $i = 1, \ldots, N$, with $\mathbf{I}^{2\times 2}$ as the identity matrix. Finally, the tracking errors are defined by

$$\begin{bmatrix} \mathbf{e}_i \\ e_{\theta_i} \end{bmatrix} = \begin{bmatrix} \mathbf{R}^T(\theta_i) & \mathbf{0}^{2\times 1} \\ \mathbf{0}^{1\times 2} & 1 \end{bmatrix} (\mathbf{q}_i^r - \mathbf{q}_i), \ i = 1, \ldots, N, \tag{10}$$

where $\mathbf{e}_i = [e_{x_i}, e_{y_i}]^T$ is the error in position, e_{θ_i} is the error in orientation, and $\mathbf{R}(\theta_i)$ is the rotational matrix respect to the GRF for the i-th robot which is given by

$$\mathbf{R}(\theta_i) = \begin{bmatrix} \cos\theta_i & -\sin\theta_i \\ \sin\theta_i & \cos\theta_i \end{bmatrix}, \ i = 1, \ldots, N. \tag{11}$$

The tracking error dynamics can be obtained by the derivative of (10) and taking in account the kinematic models of the unicycle robot (1) and the reference trajectory (7). Therefore the error dynamics are given by

$$\begin{bmatrix} \dot{\mathbf{e}}_i \\ \dot{e}_{\theta_i} \end{bmatrix} = \begin{bmatrix} \omega_i \mathbf{S}\mathbf{e}_i + \mathbf{G}_i \mathbf{V}_i \\ \omega_i^r - \omega_i \end{bmatrix}, \ i = 1, \ldots, N, \tag{12}$$

where $\mathbf{V}_i = [v_i^r, v_i]^T$ and

$$\mathbf{G}_i = \begin{bmatrix} \cos e_{\theta_i} & -1 \\ \sin e_{\theta_i} & 0 \end{bmatrix}, \ i = 1, \ldots, N. \tag{13}$$

As it can be seen, the errors on the GRF are transformed to the robot reference frame (RRF), in (10), for easing the computing of the control law, see Gutierrez et al. (2017). In the same reference, the authors define coupling errors which are given by

$$\epsilon_{x_{ij}} = e_{x_i} - e_{x_j}, \tag{14}$$
$$\epsilon_{y_{ij}} = e_{y_i} - e_{y_j}, \tag{15}$$

where $\epsilon_{x_{ij}}$ and $\epsilon_{y_{ij}}$ are the coupling errors for the x-axis and y-axis, respectively.

For each robot, the proposed controller in Gutierrez et al. (2017) is as follows

$$v_i = v_i^r \cos e_{\theta_i} + k_i^x e_{x_i} + C_i^x \sum_{j=1, j\neq i}^{N} \epsilon_{x_{ij}}, \tag{16}$$

$$\omega_i = \omega_i^r + k_i^\theta e_{\theta_i} + \frac{K}{\alpha_i} v_i^r k_i^y e_{y_i} \operatorname{sinc} e_{\theta_i} + + \frac{K}{\alpha_i} v_i^r \left(C_i^y \sum_{j=1, j\neq i}^{N} \epsilon_{y_{ij}} \right) \operatorname{sinc} e_{\theta_i}, \tag{17}$$

for $i = 1, \ldots, N$, where $\epsilon_{x_{ij}}$ and $\epsilon_{y_{ij}}$ are defined in (14) and (15), respectively, $k_i^x > 0$, $k_i^y > 0$, $k_i^\theta > 0$ are gains of the nonlinear controller for the errors in x, y and θ, respectively, $C_i^x > 0$ and $C_i^y > 0$ are the gains for the coupling errors on x-axis and y-axis, respectively, and

$$\alpha_i = \sqrt{K^2 + e_{x_i}^2 + e_{y_i}^2 + \sum_{j=1, j\neq i}^{N} \left(\epsilon_{x_{ij}}^2 + \epsilon_{y_{ij}}^2 \right)}. \tag{18}$$

for $i = 1, \ldots, N$, with $K > 0$ as a factor that avoids an indefiniteness of (17) when $e_{x_i} = e_{x_j} = e_{y_i} = e_{y_j} = 0$, $\forall\, j \neq i$. In this case α_i is also affected by the coupling errors.

The weighted sums in (16) and (17) are the static couplings on the x-axis and y-axis, respectively.

2.1 Problem statement

The controllers (16) and (17) proposed in (Gutierrez et al., 2017) consists of two parts: a static feedback for inducing tracking of a desired trajectory (the terms that contain e_{θ_i}, e_{x_i}, and e_{y_i}) and a static coupling for achieving synchronization of the robots (the terms containing $\epsilon_{x_{ij}}$, $\epsilon_{y_{ij}}$).

In this work, the objective is to replace the static couplings in (16) and (17) by a first order dynamic coupling. The reason behind this is to investigate whether the performance of the controller is improved by using dynamic couplings or not.

3. PROPOSED CONTROLLER

The proposed controller, which indeed is a modification of controller (16),(17), is described by

$$v_i = v_i^r \cos e_{\theta_i} + k_i^x e_{x_i} + C_i^x z_{x_i}, \tag{19}$$

$$\omega_i = \omega_i^r + k_i^\theta e_{\theta_i} + \frac{K}{\alpha_i} v_i^r k_i^y e_{y_i} \operatorname{sinc} e_{\theta_i}, \tag{20}$$

for $i = 1, \ldots, N$, where z_{x_i} is the coupling variable, which is dynamically generated by

$$\dot{z}_{x_i} = -\alpha_x z_{x_i} + \mu_x \sum_{j=1, j\neq i}^{N} L_{ij}^x \epsilon_{x_{ij}}, \tag{21}$$

where $\alpha_x > 0$ is a design parameter, $\mu_x > 0$ is the coupling strength, and L_{ij} denotes the weighted interaction between system i and j.

The rest of parameters in (19)-(20) are as defined in (16),(17), and α_i is redefined as

$$\alpha_i = \sqrt{K^2 + e_{x_i}^2 + e_{y_i}^2},\ i = 1, \ldots, N. \tag{22}$$

Remark 1. Note that both controllers (16) and (17) contain a static coupling: v_i contains a term depending on $\epsilon_{x_{ij}}$, whereas ω_i contains a term that depends on ϵ_{y_i}. However, in the proposed controller, see (19)-(20), the static coupling in v_i has been replaced by the dynamic coupling (21), but the static part in ω_i has been neglected, i.e. we have set $C_i^y = 0$. Therefore, with the proposed controller, the interaction between the robots is minimal.

By replacing (19)-(20) into (12), it follows that the tracking error dynamics are given by

$$\dot{e}_{x_i} = e_{y_i}\omega_i - k_i^x e_{x_i} - C_i^x z_{x_i}, \tag{23}$$

$$\dot{e}_{y_i} = v_i^r \sin e_{\theta_i} - e_{x_i}\omega_i, \tag{24}$$

$$\dot{e}_{\theta_i} = -k_i^\theta e_{\theta_i} - \frac{K}{\alpha_i} v_i^r k_i^y e_{y_i} \operatorname{sinc} e_{\theta_i}, \tag{25}$$

$$\dot{z}_{x_i} = -\alpha_x z_{x_i} + \mu_x \sum_{j=1, j\neq i}^{N} L_{ij}^x \epsilon_{x_{ij}}, \tag{26}$$

for $i = 1, \ldots, N$, and ω_i is as given in (20). Furthermore, z_{x_i} has been considered as an 'error' because when the systems synchronize then z_{x_i} converges asymptotically to zero.

3.1 Stability Analysis

The stability of the system (23)-(26) is established by the following theorem:

Theorem 1. Consider a network of N unicycle robots given by (1) with control inputs (19)-(20) and dynamic controller (26). Then, if the controller gains (k_i^x, k_i^y, k_i^θ, K and C_i^x) and the coefficients of the dynamic coupling are positive, i.e. $\alpha_x > 0$ and $\mu_x > 0$, then the origin of the close-loop dynamic (23)-(26) is globally asymptotically stable.

Proof. Let's define $\zeta(t) = [\mathbf{e}_x^T, \mathbf{e}_y^T, \mathbf{e}_\theta^T, \mathbf{z}_x^T]^T$, with $\mathbf{e}_x(t) = [e_{x_1}(t), \ldots, e_{x_N}(t)]^T$, $\mathbf{e}_y(t) = [e_{y_1}(t), \ldots, e_{y_N}(t)]^T$, $\mathbf{e}_\theta(t) = [e_{\theta 1}(t), \ldots, e_{\theta_N}(t)]^T$, $\mathbf{z}_x(t) = [z_{x_1}(t), \ldots, z_{x_N}(t)]^T$.

The stability of the system (23)-(26) can be established by the following quadratic Lyapunov function

$$V(\zeta(t)) = \sum_{i=1}^{N} \left[K k_i^y \alpha_i + \frac{1}{2} \left(e_{\theta_i}^2 + z_{x_i}^2 \right) - K^2 k_i^y \right], \tag{27}$$

where α_i is as given in (22). It can be seen that $V(0) = 0$ and $V(\zeta(t)) > 0\ \forall\ \zeta(t) \neq \mathbf{0}$, therefore (27) is positive definite.

The time derivative of (27) is given by

$$\begin{aligned} \dot{V} &= \sum_{i}^{N} \left[\frac{K k_i^y}{\alpha_i} \left(e_{x_i}\dot{e}_{x_i} + e_{y_i}\dot{e}_{y_i} \right) + z_{x_i}\dot{z}_{x_i} + e_{\theta_i}\dot{e}_{\theta_i} \right], \\ &= \sum_{i}^{N} \left[\frac{K k_i^y}{\alpha_i} \left(-k_i^x e_{x_i}^2 - C_i^x e_{x_i} z_{x_i} \right) - \alpha_x z_{x_i}^2 + \right. \\ &\quad \left. + \mu_x z_{x_i} \sum_{j=1, j\neq i}^{N} L_{ij}^x \left(e_{x_i} - e_{x_j} \right) - k_i^\theta e_{\theta_i}^2 \right]. \end{aligned} \tag{28}$$

Equation (28) can be written in a compact form as follows

$$\begin{aligned} \dot{V} &= -\mathbf{e}_x^T \mathbf{\Gamma}^{\alpha_i} \mathbf{K}^{\mathbf{x}} \mathbf{e}_x - \mathbf{e}_x^T \mathbf{\Gamma}^{\alpha_i} \mathbf{C}^{\mathbf{x}} \mathbf{z}_x - \alpha_x \mathbf{z}_x^T \mathbf{z}_x + \\ &\quad + \mu_x \mathbf{z}_x^T \mathbf{L}^{\mathbf{x}} \mathbf{e}_x - \mathbf{e}_\theta^T \mathbf{K}^\theta \mathbf{e}_\theta, \\ &= -\xi^T \mathbf{\Gamma} \mathcal{L} \xi - \mathbf{e}_\theta^T \mathbf{K}^\theta \mathbf{e}_\theta, \end{aligned} \tag{29}$$

where $\xi = \left[\mathbf{e}_x^T, \mathbf{z}_x^T\right]^T$, $\mathbf{K}^\theta = \text{diag}\left[k_1^\theta, \ldots, k_N^\theta\right]$ and

$$\mathcal{L} = \begin{bmatrix} \mathbf{K^x} & \mathbf{C^x} \\ -\mu_x \mathbf{L^x} & \alpha_x \mathbf{I}^{N\times N} \end{bmatrix}, \ \mathbf{\Gamma} = \text{diag}\left[\mathbf{\Gamma}^{\alpha_\mathbf{i}}, \mathbf{I}^{N\times N}\right],$$
$$\mathbf{\Gamma}^{\alpha_\mathbf{i}} = \text{diag}\left[\frac{Kk_1^y}{\alpha_1}, \ldots, \frac{Kk_N^y}{\alpha_N}\right], \tag{30}$$

with $\mathbf{K^x} = \text{diag}\left[k_1^x, \ldots, k_N^x\right]$, $\mathbf{C^x} = \text{diag}\left[C_1^x, \ldots, C_N^x\right]$ and $\mathbf{L^x}$ is the Laplacian matrix for the connections on the x-axis.

It can be seen that $\Gamma_{ii}^{\alpha_i} \in (0, k_i^y]$, $(i = 1, \ldots, N)$, therefore $\mathbf{\Gamma}^{\alpha_i}$ is bounded and positive definite. The matrix $\mathcal{L}$ is positive definite for $\mu_x > 0$ for all of kind of connectivities, therefore the product $\Gamma\mathcal{L}$ is definite positive. Also the matrix $\mathbf{K}^\theta$ is positive definite due to $k_i^\theta > 0$, $(i = 1, \ldots, N)$. Therefore, the system (23)-(26) is stable in terms of the tracking errors because $\dot{V}(\zeta) \leq 0 \ \forall \ \zeta = \left[\mathbf{0}^{N\times 1}, \mathbf{e}_y^T, \mathbf{0}^{N\times 1}, \mathbf{0}^{N\times 1}\right]^T$.

We now need to demonstrate that the system (23)-(26) converges globally asymptotically to zero. That's why we use the Barbalat's Lemma to prove it, see Khalil (2018). By integrating (29), we have the following bounds

$$0 \geq \int_0^\infty dV(\zeta(t)) = -\int_0^\infty \left[\xi^T \mathbf{\Gamma}\mathcal{L}\xi + \mathbf{e}_\theta^T \mathbf{K}^\theta \mathbf{e}_\theta\right] \mathrm{d}t, \tag{31}$$

where $V(\zeta(t))$ is lower bounded by the initial conditions $(\zeta(0) = [\mathbf{e_{x_i}}^T(0), \mathbf{e_y}^T(0), \mathbf{e}_\theta{}^T(0), \mathbf{z_x}^T(0)]^T)$, i.e. exists and it is finite. Considering a subset where the errors are all of them bounded, we obtain

$$\lim_{t\to\infty} \left[\xi^T \mathbf{\Gamma}\mathcal{L}\xi + \mathbf{e}_\theta^T \mathbf{K}^\theta \mathbf{e}_\theta\right] = 0, \tag{32}$$

which implies

$$\lim_{t\to\infty} \left[\|\xi\|_1 + \|\mathbf{e}_\theta\|_1\right] = 0. \tag{33}$$

It is necessary to prove that the only solution of the system (23)-(26) is $(e_{x_i}, e_{y_i}, e_{\theta_i}, z_{x_i}) = (0, 0, 0, 0)$ when $t \to \infty$. To achieve this, we use the dynamic of e_{θ_i} as in Gutierrez et al. (2017)

$$\dot{e}_{\theta_i} = -k_i^\theta e_{\theta_i} - \frac{K}{\alpha_i} k_i^y v_i^r e_{y_i} \,\text{sinc}\, e_{\theta_i}, \ i = 1, \ldots, N, \tag{34}$$

where, according to (33), $e_{x_i} = e_{\theta_i} = 0$, $(i = 1, \ldots, N)$, for $t \to \infty$. Therefore, we have

$$\lim_{t\to\infty} \dot{e}_{\theta_i} = \lim_{t\to\infty} -\frac{K}{\alpha_i} k_i^y v_i^r e_{y_i} = 0, \ i = 1, \ldots, N, \tag{35}$$

which implies that the only solution is $e_{y_i} = 0$ $(i = 1, \ldots, N)$ for which (35) is true. Therefore, we conclude that the origin of the system (12) with controls (19)-(20) is globally asymptotically stable.

4. NUMERICAL RESULTS

We conducted some simulations to compare the results between the static controller and the proposed dynamic controller in a *pair* of unicycle robots. For the simulations we consider the time interval $0 \leq t \leq 200$ $[s]$, with a time step of 1 $[ms]$ and using the Euler step as integration method. Also we use the controller gains reported in Gutierrez et al. (2017). The values for the nonlinear controllers are $k_i^x = 5$ $[s^{-1}]$, $k_i^\theta = 2$ $[s^{-1}]$, $k_i^y = 100$ $[rad/m^2]$ and $K = 1$ $[m]$ $(i = 1, 2)$, and the gains for both couplings are in Table 1.

Table 1. Gains and parameters for couplings.

Static coupling	Value	Dynamic coupling	Value
C^x $[s^{-1}]$	5	α_x $[s^{-1}]$	10
C^y $[s^{-1}]$	100	μ_x $[-]$	20
		C_i^x $[s^{-1}]$	1
		$L_{ij}^x, i, j = 1, 2$ $[s^{-1}]$	1

The desired trajectory $(\mathbf{q}_{vc})$ for the VC is a circumference whose ratio is 1 $[m]$ and a circuit period of 100 $[s]$. On the other hand, we compute the reference orientation for each robot θ_i^r by integrating the angular velocity ω_i^r due to the tangent function is a discontinuous function, i.e. $\tan\theta_i^r \in (-\pi, \pi)$ and we need the desired trajectory to be continuous. The positions of each robot are $\mathbf{p}_1 = [-0.3, 0]$ and $\mathbf{p}_2 = [0.3, 0]$ respect to the VC and their initial conditions are $\mathbf{q}_1 = [0, 0, \pi]^T$ and $\mathbf{q}_2 = [0.5, -0.5, 0]^T$.

The desired trajectory as well as the real trajectory for each robot are shown in Fig. 2 where the x markers indicate the initial conditions. These results have a perturbation in the linear velocity of the first car which simulates there is an obstacle that prohibits its linear movement. This disturbance is applied at $t = 150$ $[s]$ during 20 $[s]$.

The results corresponding to the static coupling (original controller) are depicted in Fig. 3a, whereas those obtained with the proposed controller are shown in 3b. It can be seen that in both cases the robots achieve their respective trajectories and after the perturbation the first robot describes a line and achieves its trajectory faster with the static controller compared to the dynamic controller. However, for the second robot, the things are different: with the dynamic controller the second robot achieves its trajectory faster than with the static coupling because the perturbation affects little bit to the secon robot with the dynamic coupling.

Next, we compare the tracking errors for $x-axis$ (e_{x_i}), $y-axis$ (e_{y_i}) and orientation (e_{θ_i}). These errors are shown in Fig. 3. For both couplings, the errors on $x-axis$ as shown in Figs. 3a-b. But, there are some differences for the errors on $y-axis$ and orientation between both couplings, as depicted in Figs. 3c-f. The errors e_{y_i} and e_{θ_i} $(i = 1, 2)$ are smaller with a static coupling than those with a dynamic coupling. Perhaps these differences appear due to the fact that the proposed dynamic controller only appears in v_i but not in ω_i.

On the other hand, Fig. 4 shows the synchronization errors $\epsilon_{x_{ij}}$. It can be seen that the errors converge also to zero at the beginning and during perturbation, see Fig. 4a. Furthermore, the dynamic couplings also converge to zero, as presented in Fig. 4b.

We have observed that the proposed dynamic coupling reduces the velocities (linear and angular) that each robot needs to achieve their trajectories, see Fig. 5. It can be seen that the velocities are similar for both couplings once errors converge to zero. But there are differences between both results at the beginning and during perturbation. In fact, as can be seen from Figs. 5b and 5d, the values of the instant velocities are smaller with the dynamic coupling than with the static coupling.

Finally, we perform a numerical study about the energy of the velocities v_i and ω_i (linear and angular) to determine

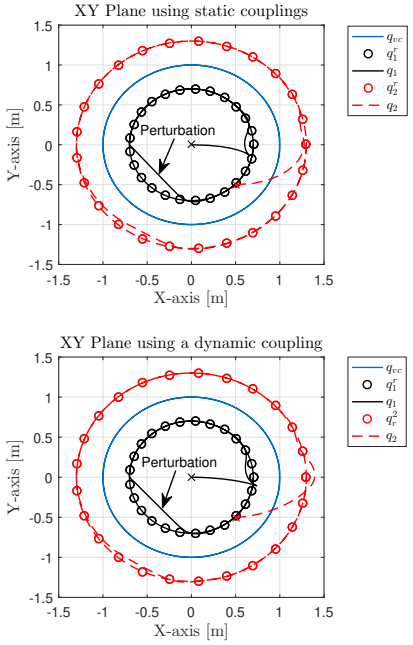

Fig. 2. XY phase plane. Panel a) Results obtained with the static controller (16)-(17). Panel b) Results for the proposed controller (19)-(20).

which coupling has the best performance from an energetic view point.

According to Oppenheim et al. (1997), we define the following energy functions to compute the energy of these signals at each instant of time.

$$E_{v_i}(t) = \int_0^t |v_i(\tau)|^2 \mathrm{d}\tau, \ i = 1, 2, \tag{36}$$

$$E_{\omega_i}(t) = \int_0^t |\omega_i(\tau)|^2 \mathrm{d}\tau, \ i = 1, 2. \tag{37}$$

The results are shown in Fig. 6. It can be seen that the energy of both velocities are smaller with the dynamic coupling than with the static coupling, even when a perturbation is applied, from 150 to 170 seconds. According with these results, we draw the conjecture that using the proposed dynamic coupling yields to a reduction in the energy required by the controller to achieve the required synchronization task.

5. CONCLUSIONS

We presented a control strategy to couple two or more unicycle robots, which allows keeping a formation while following a prescribed trajectory. The numerical results presented here suggest that the energy needed to keep the robots within the formation is smaller if the coupling between the systems is dynamic rather than static.

Another advantage of the proposed controller is that minimal interaction between the robots is required. In our previous work (Gutierrez et al., 2017), the robots were coupled via two variables. However, in the dynamic controller proposed here, the robots interact through only one variable.

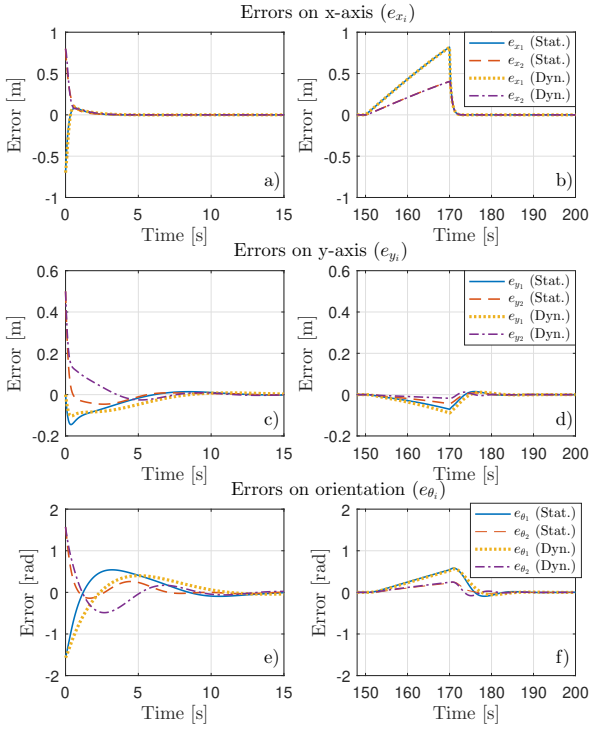

Fig. 3. Tracking errors. Left panels are for the initial errors and right panels are the errors during the perturbation.

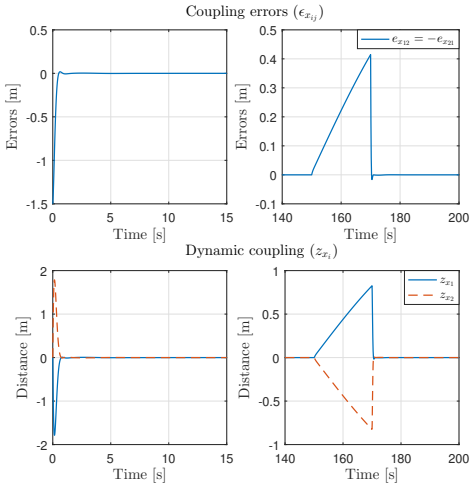

Fig. 4. Coupling errors using dynamic coupling. The left panel is for the errors at the beginning and the right panel is for the errors during perturbation.

On the other hand, the proposed controller requires to increase the number of equations in the system because at each node we have to add one extra equation for the dynamic coupling. This fact may be seen as disadvantage for a centralized distribution because the computing time may increase as the number of robots increases. It is worth mentioning that the stability proof only takes into account the tracking errors. Currently, we are extending this proof in order to also consider the synchronization errors.

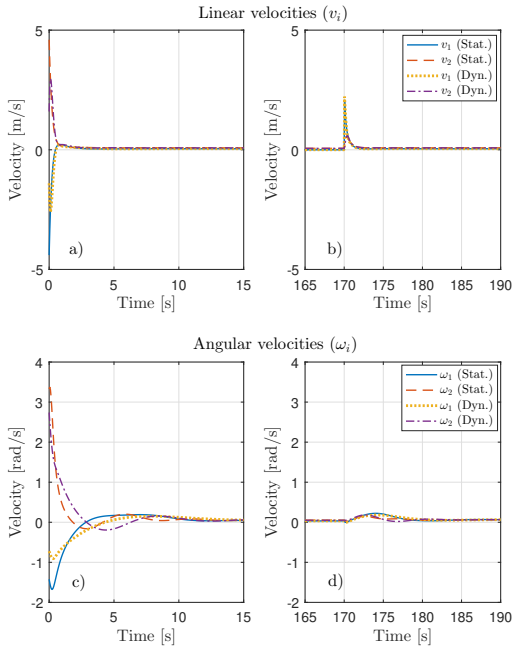

Fig. 5. Velocities for each robot. Panels a) and b) are for linear velocities at the beginning and during the perturbation, respectively, and panels c) and d) are for angular velocities. Similar to Fig. 3, left panels are for the errors at the beginning and right panels are the errors during perturbation.

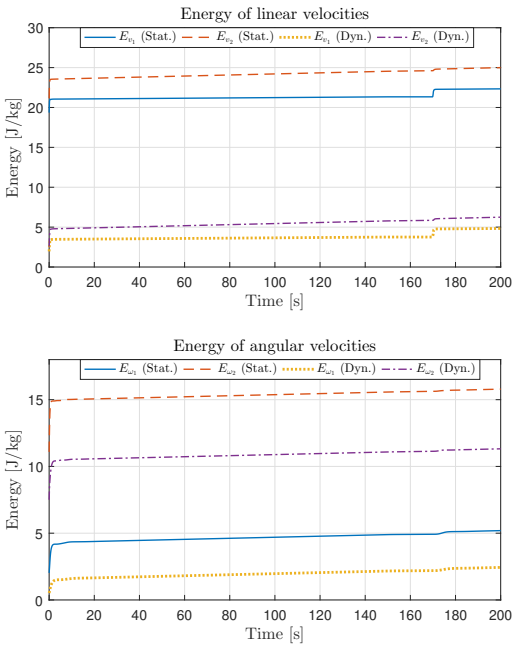

Fig. 6. Energies obtained from v_i and ω_i. Panel a) is for linear velocities and panel b) is for angular velocities. In both cases, the energy level is smaller for the case where the robots interact via the proposed dynamic controller.

ACKNOWLEDGEMENTS

The authors acknowledge the support from CONACYT, through the grant A1-S-26123: "Análisis, control y sincronización de sistemas complejos con interconexiones dinámicas y acoplamientos flexibles."

REFERENCES

Cao, Y., Yu, W., Ren, W., and Chen, G. (2013). An overview of Recent Progress in the Study of Distributed Multi-Agent Coordination. *IEEE Transactions on industrial informatics*, 9(1).

Gutierrez, H., Morales, A., and Nijmiejer, H. (2017). Synchronization control for a swarm of unicycle robots: Analysis of different controller topologies. *Asian Journal of Control*, 19(6), 1–12.

Khalil, H.K. (2018). *Nonlinear Systems*. Pearson, India, 3th edition.

Morales, A. and Nijmiejer, H. (2016). Merging strategy for vehicles by applying cooperative tracking control. *IEEE Transactions on Intelligent Transportation Systems*, 17(12), 3423–3433.

Olfati, R. and Murray, R. (2004). Consensus Problem in Networks of Agents With Switching Topology and Time-Delays. *IEEE Transactions on Automatic Control*, 49(9).

Oppenheim, A.V., Willsky, A.S., and Nawab, S.H. (1997). *Signals & Systems*. Pretince-Hall International, Inc., United States, 2dn edition.

Pavone, M. and Frazzoli, E. (2007). Decentralized policies for geometric pattern formation and path coverage. *J. Dyn. Syst. , Meas., Control*, 129(5), 633–643.

Pena Ramirez, J., Arellano-Delgado, A., and Nijmeijer, H. (2018). Enhancing master-slave synchronization: The effect of using a dynamic coupling. *Physical Review E*, 98(1), 1–10.

Pereira, T., Eldering, J., Rasmussen, M., and Veneziani, A. (2014). Towards a theory for diffusive coupling functions allowing persistent synchronization. *Nonlinearity*, 27(3), 501–525.

Ren, W. (2009). Collective motion from consensus with cartesian coordinate coupling. *IEEE Trans. Autom. Control*, 54(6), 1330–1336.

Suykens, J.A.K., Curran, P.F., and Chua, L.O. (1997). Master-slave synchronization using dynamic output feedback. *International Journal of Bifurcation and Chaos*, 07(03), 671–679.

van de Wouw, N., Lefeber, E., and Lopez Aretega, I. (2017). *Nonlinear Systems. Techniques for Dynamical Analysis and Control*, volume 470. Springer Book.